Determination of breakdown voltage along the surface of a cylindrical insulator

Determination of Breakdown Voltage along the Surface of a Cylindrical Insulator

Alexey Zhabin[1], Antoine Silvestre de Ferron[1], Laurent Ariztia[1], Marc Rivaletto[1], Bucur M. Novac[1,2] and Laurent Pecastaing[1]

(1) Laboratoire des Sciences de l'Ingénieur Appliquées à la Mécanique et au génie Electrique – Fédération IPRA, Université de Pau et des Pays de l'Adour/E2S UPPA
64000 Pau, France

(2) Wolfson School of Mechanical, Electrical and Manufacturing Engineering
Loughborough University
Loughborough, Leicestershire LE11 3TU, UK

ABSTRACT

This paper investigates the electric breakdown along the surface of a cylindrical dielectric, part of a coaxial transmission line. The particular geometry of the insulator is very common, as it is used at the input or output of most high-power, high voltage generators. The streamer propagation criterion is used to calculate the flashover voltage. Studies of the dependence of the flashover voltage on the distance between the electrodes obtained in tests with DC voltage and also by applying voltage impulses with different durations and rise-times are reported. The highest difference between the estimated values and the experimental data is less than 15%, which proves the applicability of the criterion for determining the surface breakdown voltage within the geometry under study. In particular, the results of these studies are used in the design of a compact 0.5 MV pulsed power system currently under development.

Index Terms — Flashover, Surface discharges, High-voltage techniques, Marx generators, Electric breakdown

1 INTRODUCTION

THE surface breakdown is a decisive factor in determining the maximum operating voltage of any pulsed power system since the dielectric surface has always a lower insulation strength than a pure gas gap or a bulk insulator [1]. It is therefore imperative to avoid surface flashover by proper design because otherwise this unwanted phenomenon could cause significant damage, strongly affecting the characteristics of any pulsed power system. The determination of the surface flashover voltage is a complex issue, since it depends on several factors: the properties of the solid insulating material, the nature of the surrounding gas and its pressure and humidity, as well as various geometrical parameters, such as the shape of the insulator and its adjacent electrodes [2]. Many publications dealing with the theory of surface breakdown [3, 4] describe numerical simulations made for understanding the characteristics of various simple insulator geometries [1, 2]. Several engineering design criteria, based on semi-empirical rules, were also presented in the literature [5-7]. These works concentrate on the breakdown phenomena along insulator surfaces having simple geometrical shapes and therefore the application of their findings for predicting flashover in real pulsed power generators is hardly possible, mainly because the actual detailed electric field distribution along the surface is not considered.

The present work relates to solving the issue of avoiding the flashover in the design of a Marx generator, consisting of 13 stages, with an equivalent capacitance per stage of 3.9 nF. Each stage contains a spark gap switch operated with the pressurized air. The output voltage of the generator is 0.5 MV, with a rise time of 25 ns. The generator coaxial output requires a compact dielectric having a cylindrical shape, such as the one presented in Figure 1. This geometry is very common for insulators placed at the input or output of pulsed power generators [8-13]. At the same time, this particular shape of dielectric has certain features that have to be observed in order to avoid flashover, which makes the published formulas for simple geometries not applicable for calculating the surface breakdown voltage. One essential feature is that the radial component of the electric field vector prevails along most of the insulator surface, which significantly decreases the flashover

Manuscript received on 13 September 2021, in final form 8 January 2022, accepted xx Month 20yy. Corresponding author: A. Zhabin. ***Don't edit this text box!!***

voltage [14]. Furthermore, if the flashover occurs, the discharge must propagate along the internal (S_1), end face (S_2) and external (S_3) surfaces of the cylindrical insulator, as highlighted in Figure 1. Hence, when determining the breakdown voltage, the properties of *all surfaces and the field distribution along them* should both be considered.

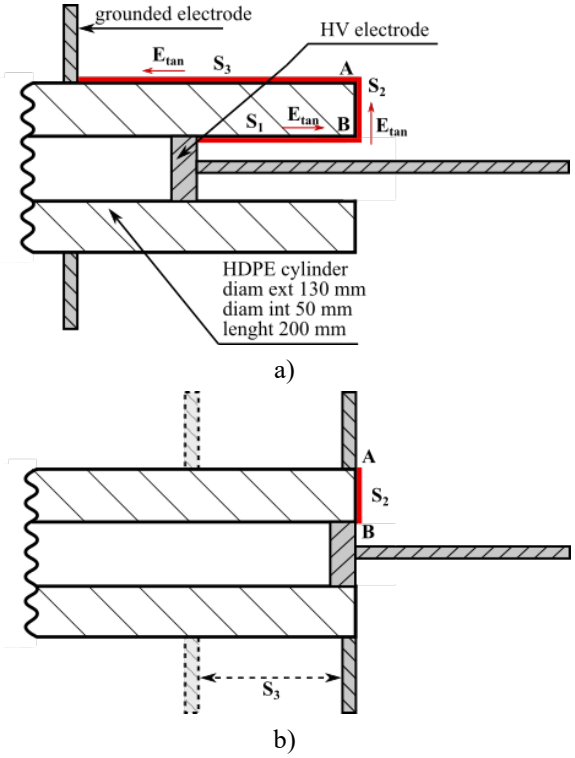

Figure 1. Mechanical design of the test bench for studying surface breakdown. Possible electric field breakdown paths are highlighted. a) general working arrangement with $S = S_1 + S_2 + S_3$, b) initial testing arrangement with $S = S_2$. The initial direction of the electric field is also shown, but this is later changing due to various processes (see text)

This paper presents results from experimental tests measuring the flashover voltage along all surfaces of the cylindrical dielectric (Figure 1a, 1b). The experimental data is then compared with the values estimated using *the streamer propagation criterion* (also known as *the equal area rule*) [15]. This criterion was previously applied to determine the breakdown voltage for other geometries [6], [16].

The paper is organized in the following way. A brief description of the surface breakdown mechanism is presented in Section II. The experimental arrangement used in the studies and the results obtained during testing are both presented in Sections III and IV, respectively. Finally, a brief section is dedicated to the main Conclusions.

2 FLASHOVER THEORY HIGHLIGHTS

The evolution of a surface breakdown consists of three stages [15]: inception, streamer propagation, and arc formation (after the conductive channel bridges the electrodes). These stages follow one after another and each of them requires the fulfilment of certain conditions.

2.1 FLASHOVER INCEPTION

After the appearance of an initial electron in an area with high electric field stress, an electron avalanche starts to develop. If a critical number N_c of electrons is generated, a self-propagating streamer head forms [6]. The inception criterion is

$$\int_0^d \alpha_{eff}(E)dl = \ln(N_{cr}) = K, \quad (1)$$

where the effective ionization coefficient $\alpha_{eff}(E)=\alpha-\eta$ if $\alpha>\eta$ and $\alpha_{eff}(E)=0$ otherwise, E is the tangential component of the electric field to the surface of the dielectric, α represents the Townsend first ionization coefficient, η is the attachment coefficient, d is the length of the flashover path and K is a constant equal to 18 [17]. The integration starts at the point of the maximum field, follows a path along the dielectric surface, and ends where the critical value of electric field E_{CR} is reached. For atmospheric air operation, E_{CR} is 26 kV/cm [16].

2.2 STREAMER PROPAGATION

If the field enhancement at the HV electrode is sufficient to fulfill the inception criterion, Equation (1), a streamer head starts to propagate towards the ground electrode. As the streamer propagates, a space charge of the avalanche induces a high electric field in front of its head in the direction of propagation. This high electric field ionizes more charge carriers, which then co-participate in the formation of a more powerful streamer. Therefore, during this phase of the discharge, a streamer represents a self-sustaining ionization wave. For a stable streamer propagation along the dielectric surface, the external electric field in front of the streamer head should exceed a certain threshold E_{ST} value [7]. A typical value of E_{ST} in the air is 5 kV/cm. However, this value can vary in the range from 4.5 kV/cm to 6 kV/cm, depending on many factors, such as the relative permittivity of the dielectric material [7], the level of applied voltage [16], and its polarity [6], etc.

2.3 ARC FORMATION

The inception of a streamer and the beginning of its propagation does not mean that a flashover takes place. The streamer can propagate along a surface over a distance of more than 10 cm without however reaching the ground electrode. The voltage value that enables a streamer to reach the ground electrode, flashover voltage (V_{FL}), can be found from the following formula [6]:

$$V_{FL} = V_0 + d \cdot E_{ST} \quad (2)$$

where V_0 is the excess potential needed to generate a breakdown once the streamer connects the two electrodes. It can take values in the range from 20 kV to 30 kV (for example V_0 = 24 kV in [15] and V_0 = 23.7 kV in [16]).

3 EXPERIMENTAL ARRANGEMENT

A test bench was assembled to investigate the flashover phenomenon along the surface of an insulator with cylindrical symmetry. The mechanical design of the test bench is presented

in Figure 1. Two types of HV sources were used during testing: a DC source and a pulse generator, producing lightning impulses of either 0.1/1.4 μs or 1.2/50 μs.

3.1 TEST BENCH

The test bench in Figure 1 represents a scaled-down version of the Marx generator HV output, with the parameters S_i *(i* = 1,2,3*)* as indicated. By maintaining the distance S_2 = 4 cm fixed, the total length of the discharge path along the dielectric surface S can be varied by changing the relative positions of the HV and ground electrode from 4 cm to 27 cm. The insulator was made from high-density polyethylene HDPE 1000, having a dielectric constant of 2.3. The dielectric surface was in contact with the atmospheric air during all tests. The humidity of the air was in the range from 55% to 65%. The electrodes were made from stainless steel and were finely polished and carefully cleaned. The HV electrode has a cylindrical shape with a diameter of 5 cm and a height of 1 cm. It was supplied as a thin (0.5 cm in diameter) metal rod (Figure 3) with a length of 80 cm that exceeded the dimensions of all S_i. Prior to testing, the dielectric was rinsed in isopropyl alcohol and dried in an oven at 50 °C for one hour to remove all surface moisture. Powder-free latex gloves were worn throughout this treatment process to prevent re-contamination of the surfaces. A grounded copper wire mesh was used to remove any residual charges before each test. During the experiments, no irreversible changes of the surface of the dielectric were observed.

Various electric breakdown tests were conducted with electrodes positioned in different arrangements, with the assembly fixed with the aid of a tripod. First, the arrangement shown in Figure 1b was used. The HV electrode is fixed at point B, while the ground electrode is initially installed at point A (S_1 = 0, $S = S_2$ = 4 cm, S_3 = 0) and then repositioned at various distances with an increment of 1 cm ($S = S_2 + S_3$). Then, tests were performed with arrangement presented in Figure 1a ($S = S_1 + S_2 + S_3$) with two electrodes positioned at various distances as detailed in the figure. The flashover event was clearly determined by observing a very fast variation in both the voltage and the current waveform. During experiments, the distance was increased until a flashover was not observed.

The electric field along the insulator surface flashover path highlighted in Figure 1a was analyzed to predict the flashover. The field distribution was obtained using the CST Studio Suite software [18] and is presented in Figure 2. As expected, the distribution has a maximum near the HV electrode at the triple point area. The electric field has a minimum near point A for most possible electrode arrangements. If the parameter S_1 has a small value (S_1 < 3 cm), and the parameter S_3 is relatively large (S_3 > 11 cm), the lowest electric field is on the surface S_3.

The electrostatic simulation also determined the voltage of streamer inception for all positions of two electrodes. This voltage corresponds to the electric field required to meet the condition of Equation (1). Next, the voltage at which the field distribution along the dielectric surface exceeds the threshold E_{ST} required for a stable streamer propagation was found. As a first procedure, the highest value between these two voltages was decided to be considered as the flashover voltage V_{FL} and this value was then compared with the experimental results. This analysis has been conducted for all the possible relative positions of the electrodes (i.e., S_1 and S_3 varied in the range from 0 cm to 14 cm while S_2=4 cm was a constant). As presented below in Figures 6 and 7, this method did not always provide estimates very close to experimental data. As appears from the graphs, there were instances for which a significant difference was observed (e.g., up to 25%) with the difference rising with the inter electrode distance. Such results can be explained by the fact that the initial distribution of the electric field undergoes significant changes due to the presence of space charges in the streamer head. Since the streamer, while propagating, is capable to ionize the gas in front of its head and maintain the electric field at a sufficiently high level (E_{ST}), it was decided to only use the streamer propagation criterion (2) for determining the flashover voltage. The voltage values calculated using this second methodology exceed the voltage values for the streamer inception for all the relative positions of the two electrodes. The next Section will present a comparison between the surface breakdown voltages estimated this way with the experimental data.

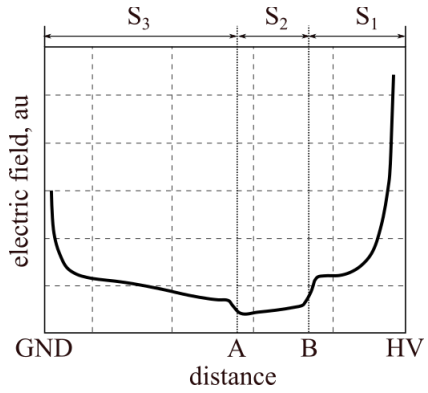

Figure 2. Electric field distribution along the electric breakdown path highlighted in Figure 1a.

3.2 EXPERIMENTS WITH HV DC

The equivalent electrical circuit of the arrangement used for measuring the flashover voltage under HV DC conditions is shown in Figure 3a. A 100 kV HV DC charger (SPELLMAN SL1200) was used. A current-limiting 1 kΩ-resistor R_1 was placed in series with the voltage supply to protect the surfaces of both the insulator and the electrode from any damage by high-current arcing and thus to avoid any possible influences on the subsequent flashover experiments. The applied voltage was monitored using a NORTHSTAR PVM 100 [19] voltage probe VP_1. A current monitor PEARSON Model 101 [20] was used to measure the discharge current CP_1. A typical pair of voltage and current waveforms recorded during a test is shown in Figure 4. Before the breakdown occurs, the voltage on the HV electrode remains almost constant. An abrupt drop in voltage and a rapid increase of the discharge current indicate the breakdown voltage is reached, with fast damped oscillations being generated afterwards.

The *Raising method* [21] was used to accurately determine the flashover voltage. This method requires the insulator to be subjected to an electric stress corresponding to 80% of the estimated flashover voltage, as determined from the previous trials. The applied voltage increases steadily with a rate of 0.5 kV/s until a flashover is obtained. The measurements are repeated 8 times and then an average value is calculated. The standard deviation of the flashover voltage is less than 10%.

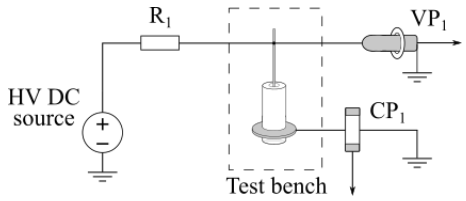

(a) Equivalent electrical circuit of the practical arrangement used during testing with HV DC

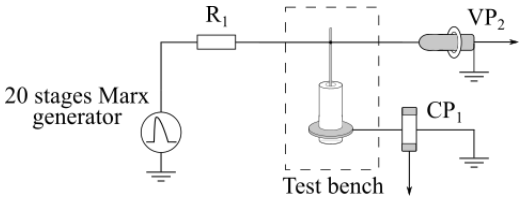

(b) Equivalent electrical circuit of the practical arrangement used during testing with 1.2/50 μs lightning impulse

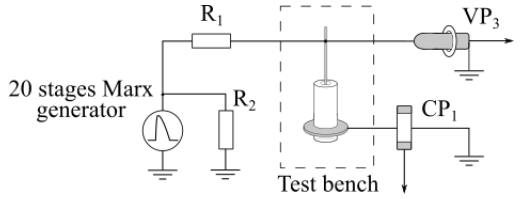

(c) Equivalent electrical circuit of the practical arrangement used during testing with 0.1/1.4 μs lightning impulse

Figure 3. Equivalent electrical circuits for all arrangements used in measuring the flashover voltage.

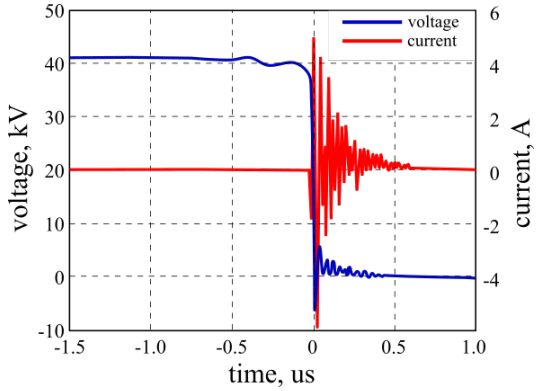

Figure 4. Typical voltage and current waveforms for an experiment using a HV DC source.

3.3 EXPERIMENTS WITH HV LIGHTNING IMPULSES

The lightning impulse tests used a 20-stage Marx generator (Figure 3b). The Marx is powered using the same 100 kV HV DC voltage charger as described above. Two types of impulses can be produced by the Marx generator. Slow impulses of 1.2/50 μs up to 200 kV are measured using an in-house manufactured capacitive voltage divider VP_2. Typical voltage and current waveforms of lightning tests are presented in Figure 5. Flashover takes place 2 μs to 4 μs after applying the lightning impulse, with an abrupt drop in voltage signal and a very fast variation in the discharge current waveform. Test impulses of 0.1/1.4 μs up to 150 kV require a 36 Ω resistor R_2 to be connected in parallel with the Marx output with the output voltage monitored using a high bandwidth voltage probe NORTHSTAR PVM 100 [19] VP_3 (Figure 3c). In both cases, the current is monitored using the same current probe CP_1 as detailed above.

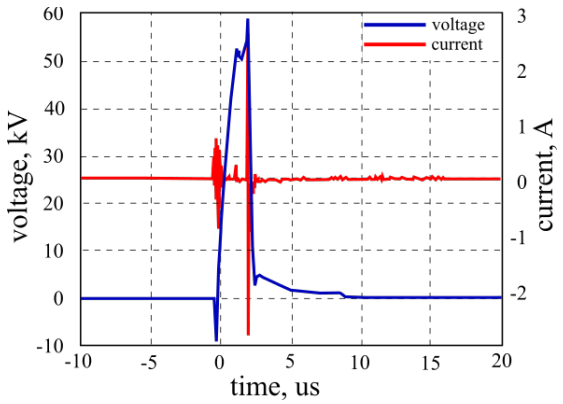

Figure 5. Typical voltage and current waveforms for an experiment using the lightning impulse source.

The "*Up and Down*" method [22] was used to obtain the experimental flashover voltage value. First, the pulse amplitude was generated to be slightly less than the expected flashover voltage. The amplitude of the next pulse was increased by ΔV, if there was no flashover in the previous test, and decreased by ΔV if flashover was observed. The total number of shots in a test sequence has been arbitrarily fixed to 10. The value of ΔV was set to 5 kV, which is 10% of the lowest flashover voltage measured in the tests. The experimental breakdown voltage is finally obtained as an average of all values determined during the tests.

The full collection of data obtained in experiments with HV lightning impulses of different durations was used to obtain the relationship between the pre-breakdown time delay and the intensity of the flashover electric field.

4 EXPERIMENTAL RESULTS

4.1 RESULTS WITH DC HV

The variation of the flashover voltage with the total length of the discharge path S along the dielectric surface is presented in Figure 6. The dependence was obtained for the values of S_1 in the range from 0 to 5 cm while S_3 was varied from 0 up to the value at which no surface breakdown occurred. As the HV DC source has a limit of 100 kV, when S_1 was further increased, it was only possible to obtain two points (or even only one). As demonstrated by the data in Figure 6, the flashover voltage

increases linearly with S. The same figure also shows the dependence of the flashover voltage on the distance between the electrodes when calculated using Equation (2). The most significant difference between the experimental data and the calculated values takes place at $S_1 = 0$. The reason for this difference is the electric field enhancement due to the sharp edge of the HV electrode when it is in point B (see Figure 1b). For other positions of the HV electrode, the difference between the calculated and experimental values is less than 15%. The best approximation of the test results with Equation (2) was obtained for $E_{ST} = 5.2$ kV/cm and $V_0 = 26.5$ kV.

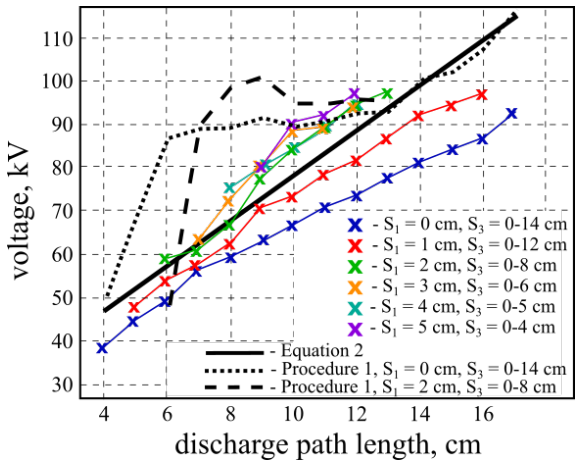

Figure 6. Flashover voltage for different electric discharge path lengths when DC voltage is applied.

4.2 RESULTS WITH LIGHTNING IMPULSE

The variation of the flashover voltage with the inter-electrode distance when a lightning impulse is applied is shown in Figure 7. The experimental results have the form of a linear function. The surface breakdown voltages measured in the experiments with slow lightning impulses (i.e., 1.2/50 μs) have lower values when compared with those obtained in tests with faster impulses (i.e., 0.1/1.4 μs). For slow pulses, the flashover voltages for lightning impulses were determined for the entire range of distance between the electrodes when S_1 and S_3 vary between 0 cm and 14 cm. However, for reasons related to clarity, only flashover voltages for the following collection of S_1 are presented in Figure 7: 0, 2, 4, 8, 10, and 13 cm. During tests for fast impulses, measurements of the flashover voltage were limited by the voltage probe maximum voltage. Therefore breakdown voltage values were obtained only for the values of S_1 in the range from 0 to 2 cm while S_3 was varied from 0 up to the value at which no surface breakdown occurred. As can be seen in Figure 7, the experimental data of both impulses is in good agreement with the estimation provided by Equation (2), with differences being less than 15% for the entire range of distances between the two electrodes. Thus, it can be concluded for the insulator geometry considered in this work, the streamer propagation criterion can be successfully used in obtaining a credible estimation for the flashover voltage. Both E_{ST} and V_0 were determined from the experimental data as 6 kV/cm and 24 kV, respectively, for slow lightning impulses, and 19 kV/cm and 27 kV, respectively for fast impulses.

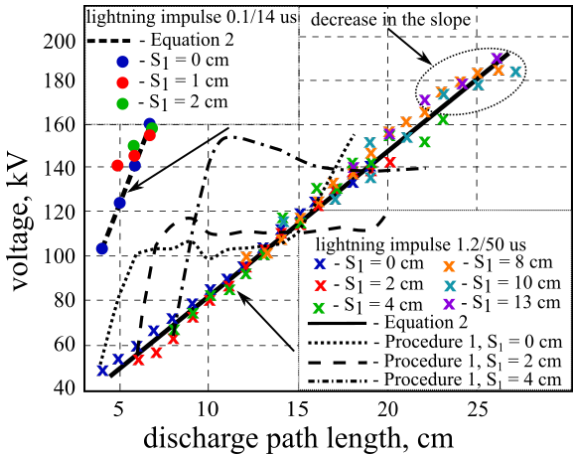

Figure 7. Flashover voltage for different electric discharge path lengths when a lightning impulse is applied having the time characteristics: solid line (Equation (2)), crosses, experiments with 1.2/50 μs, dotted line (Equation (2)), circles, experiments with 0.1/1.4 μs.

The dependences of the flashover voltage in Figure 7 slightly changes the slope if the applied voltage exceeds 170 kV and the distance between the electrodes is larger than 23 cm. This phenomenon can be explained as follows: with an increase in the distance between the electrodes, the normal component of the electric field applied to the dielectric surface starts to prevail over the tangential component. For such configurations, the propagating discharge channel is additionally fed by displacement currents that close the circuit via the capacitance formed by the channel and the ground electrode [14]. This causes the plasma temperature and conductivity inside the plasma channel to rise. As a result, the surface discharge propagation is facilitated and the slope of the voltage versus distance curve decreases. The decrease in the slope, highlighted in Figure 7, can be associated with the beginning of the streamer-leader transition. Thus, it can be hypothesized that with a further increase in the distance between the electrodes, the application of Equation (2) provides higher values of flashover voltage than ones observed during experiments.

Figure 8 presents the variation of the pre-breakdown time delay with the applied flashover electric field, where the pre-breakdown time delay is considered as the time interval from the beginning of the impulse voltage until the completion of the flashover and where the electric field strength is defined as the ratio of the flashover voltage to the total flashover path along the insulator. Figure 8 is supplemented with data taken from [23] to include the nanosecond range (i.e., less than 0.1 us). The experimental data can be best matched using a power function $f(t_p)=a \cdot t_p^b$, where $a = 0.15 \cdot \text{kV} \cdot \text{s}^{0.32}/\text{cm}$ and $b = -0.32$. It is obvious that, if a longer impulse is applied, the breakdown along the surface occurs for lower values of the electric field strength. It could be noted as well that the average value of the flashover electric field for shorter lightning impulses (25 kV/cm) is 3.1 times higher than for longer

impulses (8 kV/cm). For the same impulses the same ratio is obtained for the E_{ST} values: 19 kV/cm and 6 kV/cm, respectively.

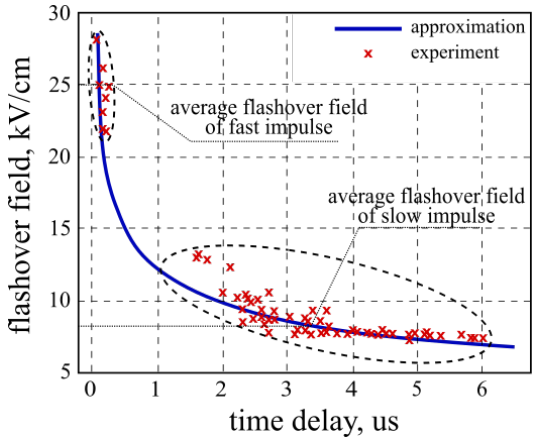

Figure 8. The relationship between the pre-breakdown time delay and the applied flashover electric field

5 FINAL DESIGN AND MANUFACTURE OF THE 500 KV MARX OUTPUT

The LTspice simulation of the electrical circuit of the Marx generator was carried out. Details about the generator design and simulation features will be presented elsewhere. The predicted waveform of the voltage on a 140 Ω load is presented in Figure 9. It is easy to note the voltage impulse reaches a 500 kV peak with a rise time of 25 ns. Using this result, the time interval of 200 ns was considered as the pre-breakdown time delay in the calculations, to completely avoid flashover along the surface of the dielectric. As a consequence, using the graph in Figure 8 and for a pre-breakdown delay of 200 ns, the flashover field is estimated to be 20.88 kV/cm. This value is 2.61 times higher than the average one for a slow pulse highlighted in Figure 8. It follows that the electric field strength required for streamer propagation is 15.3 kV/cm. In this case, the height of a cylindrical dielectric with a thickness of 4 cm should exceed 15.5 cm.

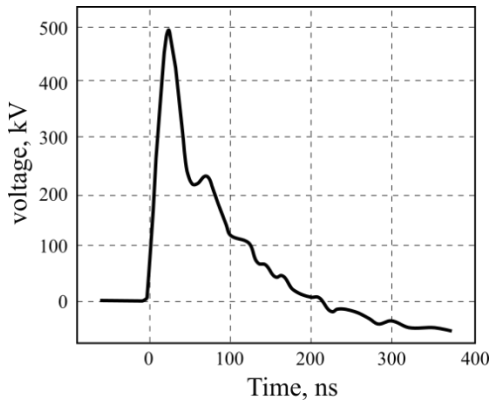

Figure 9. Theoretical prediction for the output voltage impulse of the Marx generator when coupled to a 140 Ω resistive load

However, as was mentioned above, the increase of streamer conductivity will take place due to the long surface breakdown discharge length and the high applied voltage. Thus, the actual flashover voltage of the dielectric surface will be lower than the calculated value. Therefore, the dimensions of the insulator at the output of the generator were increased to the values shown in Figure 10a to avoid flashover. A photo of the final design is shown in Figure 10b.

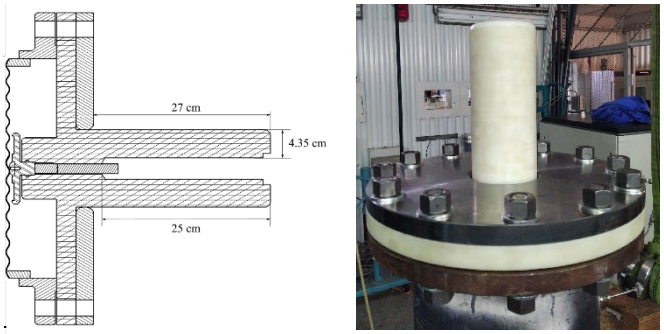

(a) (b)

Figure 10. Marx generator HV output: a) design characteristics; b) photo of the real unit

6 CONCLUSIONS

The electric field breakdown along the surface of an insulator, part of a HV coaxial output of a 0.5 MV pulsed power generator, was studied to establish the optimum design criteria. The tests were carried out for various distances between the electrodes in the interval 4 cm to 27 cm with the electrodes placed in different relative positions to provide different electric field distributions along the insulator surface. The tests demonstrated the flashover voltage increases linearly with the inter-electrode distance. The streamer propagation condition was used to calculate the surface breakdown voltage, with the estimations being in good agreement with the experimental data i.e., a difference lower than 15%. Thus, one of the conclusions of the present work is that the *flashover voltage* for the considered experimental conditions seems to *only depend on the fulfillment of the streamer propagation condition*.

Based on experimental data, the dependence of the pre-breakdown time delay on the applied electric field was also determined. This dependence is well approximated by a power function. This curve allows to estimate the flashover voltage for impulses having different durations.

The results of the studies presented in this work allowed the precise design and successful testing of the output insulator used in a compact 0.5 MV pulsed power system currently under development. Full details related to this system will be presented elsewhere.

ACKNOWLEDGMENT

This research was carried out under the framework of E2S UPPA (PULPA chair) supported by the "Investissements d'Avenir", a French programme managed by ANR (ANR-16-IDEX-0002).

REFERENCES

[1] L. Liu *et al*., "Criteria and propagation processes of electrode-initiated and electrodeless-initiated discharge in SF6," Phys. Plasmas., vol. 26, no. 2, p. 023512, Feb. 2019.

[2] M. E. A. Slama, A. Beroual and A. Haddad, "Surface Discharges and Flashover Modelling of Solid Insulators in Gases," Energies, vol. 13, no. 3, pp. 591, Jan. 2021.
[3] A. S. Pillai and R. Hackam, "Surface flashover of solid dielectric in vacuum," Journal of Applied Physics, vol. 53, iss. 4, pp. 2983-2987, April. 1982.
[4] H. Naruse and O. Yamamoto, "Estimation of flashover voltage along cylindrical insulator in vacuum," *2014 Int. Symp. on Disch. and Elec. Ins. in Vac. (ISDEIV),* Mumbai, India, 2014, pp. 65–68.
[5] T. Yamashita *et al*, "Estimation of surface breakdown voltage of solid/gas composite insulation with embedded electrode," IEEE Trans. Dielectr. Electr. Insul., vol. 23, no. 5, pp. 3026-3033, October. 2016.
[6] A. Pedersen *et al*., "Streamer inception and propagation models for designing air insulated power devices," *2009 IEEE Conference on Electrical Insulation and Dielectric Phenomena,* Virginia Beach, VA, USA, 2009, pp. 604-607.
[7] N. L. Allen and P. N. Mikropoulos, "Streamer propagation along insulating surfaces," IEEE Trans. Dielectr. Electr. Insul., vol. 6, no. 3, pp. 357-362, June. 1999.
[8] T. Huiskamp, E. J. M. van Heesch and A. J. M. Pemen, "Final Implementation of a Subnanosecond Rise Time, Variable Pulse Duration, Variable Amplitude, Repetitive, High-Voltage Pulse Source," IEEE Trans. on Plasma Sc., vol. 43, no. 1, pp. 444-451, Jan. 2015.
[9] M. Wang *et al.*, "Bipolar Modulation of the Output of a 10-GW Pulsed Power Generator," IEEE Trans. on Plasma Sc., vol. 44, no. 10, pp. 1971-1977, Oct. 2016.
[10] L. Pecastaing *et al.*, "Very Fast Rise-Time Short-Pulse High-Voltage Generator," IEEE Trans. on Plasma Sc., vol. 34, no. 5, pp. 1822-1831, Oct. 2006.
[11] L. Pecastaing *et al.*, "A 250kV-300ps-350Hz Marx generator as source for an UWB radiation system," *2009 IEEE Pulsed Power Conference,* 2009, pp. 51-56.
[12] P. Yan, T. *et al.*, "Experimental investigation of surface flashover in vacuum using nanosecond pulses," IEEE Trans. Dielectr. Electr. Insul., vol. 14, no. 3, pp. 634-642, June. 2007.
[13] G. A. Mesyats *et al.*, "Generation of high-power subnanosecond pulses," Ultra-Wideband Short-Pulse Electromagnetics 4 (IEEE Cat. No.98EX112), pp. 1–9, 1998.
[14] V. Y. Ushakov, Insulation of High-Voltage Equipment, Springer-Verlag Berlin Heidelberg, 2004.
[15] M. Bastiaan, and Jean-René Poirier, eds, Scientific computing in electrical engineering, SCEE 2010. Vol. 16. Springer Science & Business Media, 2012.
[16] F. Mauseth, J. S. Jørstad, and A. Pedersen, "Streamer inception and propagation for air insulated rod-plane gaps with barriers," *2012 Annu. Rep. Conf. Electr. Insul. Dielect. Phenom. (CEIDP),* 2012, pp. 739-732.
[17] A. Chvyreva *et al.*, "Raether–Meek criterion for prediction of electrodeless discharge inception on a dielectric surface in different gases," J. Phys. D: Appl. Phys, vol. 5, no. 11, Feb. 2018.
[18] Computer Simulation Technology, Available: https://www.3ds.com/.
[19] North Star, Available: https://www.highvoltageprobes.com/products/high-voltage-probes.
[20] Pearson Electronics, Available: https://pearsonelectronics.com/products/wideband-current-monitors.
[21] X. Jiang *et al.*, "Study on the Influence of Test Methods on AC and DC Pollution Flashover Performance of Different UHV Insulators," PRZEGLAD ELEKTROTECHNICZNY, vol. 3, pp. 166-170, Mar. 2013.
[22] H. Raether, Electron Avalanches and Breakdown in Gases, Washington: Butterworths, 1964.

Alexey Zhabin was born in Voronezh, USSR, in 1988. He received the BSc and MSc degree from the Voronezh State University, Voronezh, Russia, in 2009 and 2011, respectively and the PhD degree from the Voronezh State Technical University, Voronezh, Russia in 2017. From 2015 to 2020, he was an Assistant Professor with the Electronic Department, Voronezh State University. He is currently a postdoctoral researcher at the SIAME Laboratory, University of Pau. His research interests are mainly focused on ultrashort pulse generation, UWB radar and telecommunication systems, pulsed power systems.

Antoine Silvestre de Ferron was born in Tarbes, France, in 1977. He received the master's degree in electrical and electronic engineering from the University of Toulouse, Toulouse, France, in 2002, and the Ph.D. degree in electrical engineering from the University of Pau, Pau, France, in 2006., From 2006 to 2008, he was a Researcher with the Atomic Energy Commission (CEA), a French government-fund technological research organization in Le Barp, France. He is currently an Engineer with the SIAME Laboratory, University of Pau. His research interests include pulsed power generation, with military and civil applications and the high-voltage transient probes associated.

Laurent Ariztia was born in Bayonne, France, in 1996. He received the BSc and MSc degree from the Université de Pau et des Pays de l'Adour (UPPA), Pau, France, in 2017 and 2019, respectively. He is currently an Engineer at the SIAME Laboratory, University of Pau. His research interests are mainly focused on pulsed power systems, such as Marx generators, and pulse forming lines for military and civil applications.

Marc Rivaletto was born in Tarbes, France, in 1960. He graduated from the Supelec Electrical Engineer School, Gif-sur-Yvette, France, in 1984, and the Ph.D. degree in electrical engineering from Pau University, Pau, France, in 1997., He is currently a Lecturer at Pau University and works in the SIAME Laboratory. His research interests are HPM sources, compact pulsed power systems, including pulse forming lines, compact Marx generator, and resonant transformer.

Laurent Pecastaing (M'13-SM'17) he received the Ph.D. and Research Directorship Habilitation degrees in electrical engineering from the Université de Pau et des Pays de l'Adour (UPPA), Pau, France, in 2001 and 2010, respectively. He is currently a Full Professor in pulsed power with University of Pau. He is the director of the SIAME laboratory and he is also the Director of a Common Laboratory between UPPA and CEA, France. His current research interests include high-power microwave sources, compact pulsed power systems, and ultrafast transient probes. Dr. Pécastaing was the Chairman of the next EAPPC/BEAMS/MEGAGAUSS Conference in France in 2021. He is also a member of the International Steering Committees for both the BEAMS Conferences and the Euro-Asian Pulsed Power Conferences.

Bucur M. Novac (M'06 – SM'08) received the M.Sc. and Ph.D. degrees in 1977 and 1989, respectively, both from the University of Bucharest. He joined the Loughborough University, UK in 1998 and is currently Professor of Pulsed Power. His research interests include compact and repetitive high-power systems, explosively and electromagnetically driven magnetic flux compression generators and their applications, electromagnetic launchers, ultrafast magneto and electro-optic sensors and 2-D modeling of pulsed-power systems. He has co-authored two books on explosive pulsed power and has published more than 200 refereed papers and conference contributions.

He is a member of the International Steering Committees for both the MEGAGAUSS Conferences and for the Euro-Asian Pulsed Power Conferences. Prof. Novac was a voting member of the Pulsed Power Science & Technology Committee in the IEEE Nuclear and Plasma Science Society and a member of the organizing committee for the IEEE International Power Modulator and High Voltage Conference as well as co-chairman of the UK Pulsed Power Symposia.

Prof. Novac is a Fellow of the Royal Academy of Engineering, a Chartered Engineer and a Fellow of The Institution of Engineering and Technology, UK.